STM JOURNALS

Journal of
Geotechnical Engineering

ISSN: 2394-1987
Volume 13, Issue 1, 2026
January–April
DOI (Journal): 10.37591/JoGE

https://journals.stmjournals.com/joge

Research JoGE

A Shear Strength Reduction Method for an Open Pit Slope Stability Analysis Based on the Finite Element Method

Dasmani Abdulai[1,*], Michael Affam[2]

Abstract

Slope stability assessment of open pit mines is critically important, since it forms part of the overall productivity and safety management strategy of the mines. This work aims to investigate the overall stability conditions of three (3) open pits in Gold Fields Limited, Tarkwa, Ghana. Field and laboratory investigations were conducted, as well as empirical methods. Finite element analysis (FEA) in Rocscience was carried out using the shear strength reduction technique. Results from the analysis revealed that the design planned for the pit walls was stable, with the critical strength reduction factor (SRF) of 5.45, 5.3, and 2.6, respectively, for Akontasi, Pepe, and Teberebie. However, critically and actively unstable zones, including potential failure mechanisms involving the oxides, transition, and the fresh rocks, have been revealed. From the analysis, there is potential for progressive failures in the pits. These will be propagated from the critical zones in the rocks. However, to ensure safe and efficient mining operations and optimize cost-effectiveness, targeted dewatering systems, especially dewatering wells and grout curtains, should be installed in the critical deformation zones to reduce water influxes, infiltration, and seepage into the pits. Also, effective monitoring programs should be intensified in the pit faces to avert any potential failure in the future.

Keywords: Finite element analysis, Rocscience, slope stability, shear strength reduction factor

INTRODUCTION

The mining industry contributes hugely to the achievements of the Sustainable Development Goals (SDGs) and therefore operates in alignment with environmental, social, and governance stewardship (ESG). More importantly, the mining enterprise is a significant driver of socio-economic advancement worldwide through infrastructure development and job creation. Therefore, as stated by scholars, e.g., Mirzehi and Moradi Afrapoli [1], a comprehensive approach including the integration of economic development, environmental stewardship, and social welfare is required to pursue the SDGs in mining enterprises. Moreover, the increasing importance of sustainability has led to the incorporation of environmentally and socially responsible principles into modern mine design, ensuring that mining operations are aligned with the principles of sustainable development [2, 3].

As highlighted by scholars, e.g., Xu et al. [3], sustainable mining practices encompass five key aspects: economic viability, environmental stewardship, community engagement, safety protocols, and operational efficiency. Despite the importance of these factors, integrating them into the mining industry's internal decision-making processes is a daunting task.

***Author For Correspondence**
Dasmani Abdulai
E-mail: dasabdul84@gmail.com

[1]Student, Department of Geological Engineering, Faculty of Geosciences and Environmental Studies, University of Mines and Technology, Tarkwa, Ghana
[2]Professor, Department of Geological Engineering, Faculty of Geosciences and Environmental Studies, University of Mines and Technology, Tarkwa, Ghana

Received Date: January 16, 2026
Accepted Date: January 21, 2026
Published Date: January 28, 2026

Citation: Dasmani Abdulai, Michael Affam. A Shear Strength Reduction Method for an Open Pit Slope Stability Analysis Based on the Finite Element Method. Journal of Geotechnical Engineering. 2026; 13(1): 1–24p.

© STM Journals 2026. All Rights Reserved

Also, while the mining sector endeavors to attain the SDGs, it presents harmful economic, environmental, social, and governance impacts if it's not pragmatic in its operations, especially in slope stability management.

Scholars have indicated that slope stability is an integral component of the Slope Management Plan (SMP). Modeling and prediction of slope instability are important phases of the SMP, utilized by mine practitioners at both design review and operational stages of a mine's life to categorize the risks of a mine slope. Different approaches have been proposed and used by experts and scholars to model mine slope stability. The limit equilibrium methods have been utilized and are still in use in mine slope stability modeling [4–6]. However, experts and scholars, e.g., Raghuvanshi (2019) [7], pinpointed some factors affecting the factor of safety (FOS) in the limited equilibrium methods, including the geometry of the slope, failure plane characteristics, water forces, and external triggering factors.

To overcome the shortcomings of the limit equilibrium methods, numerical methods have been developed and utilized for mine slope modeling [8, 9]. In literature, the finite difference method (FDM), finite element method (FEM), boundary element method (BEM), distinct element method (DEM), discontinuous deformation analysis (DDA), and bonded particle model (BPM) are employed in numerical modeling, having the ability to handle material heterogeneity, non-linearity, and boundary conditions.

Precisely, authors have indicated some power and flexibility regarding the FEM, as it eliminates a priori assumptions on the shape and location of failure surfaces, eliminates assumptions regarding the inclinations and locations of interslice forces, can model progressive failure, calculate deformations at slope stress levels, and is robust enough to perform successfully under a wide range of conditions.

This study aimed to assess the stability conditions of Gold Fields Ghana Limited, Tarkwa, using input parameters from geological and geotechnical investigations. Based on studies, e.g., Pigois et al. (2003) and Seidu et al. (2023) [10, 11], the study area is composed of three lithological units, including conglomerates, quartzites, and phyllites, hosted in the Banket Series in the Tarkwa Concession area.

Also, intrusive rocks such as dykes and sills penetrated these sedimentary units, which are weathered. Structurally, the major features found on the mine site are characterized by sub-vertical features, intersecting the mine slopes at various points, with varying continuities, depending on the degree of disturbance within the slope areas. Experts and scholars identified the varying continuities of these features to impact the stability conditions of the mine slopes. Also, these features provide pathways for groundwater migration. Moreover, the degradation of infill materials within these structures has been pointed out as a primary cause of instability in the pit faces.

Therefore, detailed geological mapping and slope stability analysis were conducted to ascertain the safety conditions of the mine pits. Geological mapping based on systematic mapping was employed in Akontasi, Pepe, and Teberebie pits to obtain structural characteristics, failure modes, groundwater seepages, and shear zones in the pit faces. However, finite element analysis (FEA) is based on the stress reduction factor (SRF) to determine the stability conditions of the slopes, for optimization purposes.

THE CASE STUDY AREA

Overview

The Tarkwa Gold Fields are located near the town of Tarkwa (Figure 1), characterized by distinct ridges, influenced by the underlying geological structure. The drainage system in the area is mainly tributaries flowing westwards. The average yearly precipitation in the Tarkwa area is approximately 2030 mm, with a variable rainfall pattern. Studies, e.g., Avane and Saayman AF (2007) and Seidu and Ewusi (2018) [12, 13] revealed that the mine area complex structural geology and extreme rainfall patterns pose enormous challenges to the design and maintenance of stable slopes and pit depressurization (Figure 1).

© STM Journals 2026. All Rights Reserved

Journal of Geotechnical Engineering
Volume 13, Issue 1
ISSN: 2394-1987

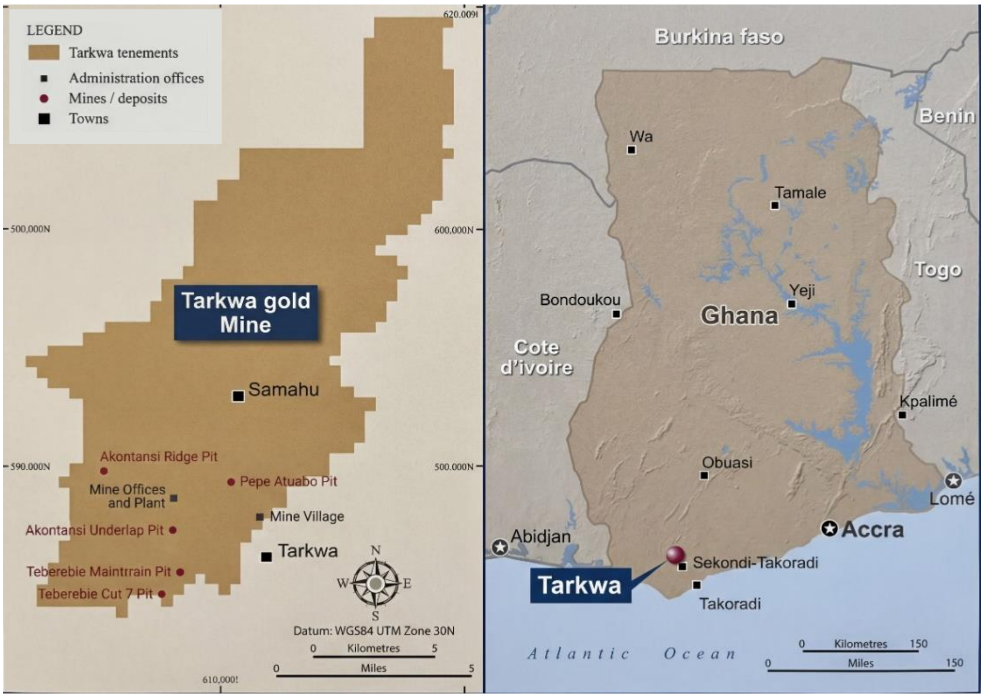

Figure 1. Location map of Tarkwa and the gold fields gold mine (after [14]).

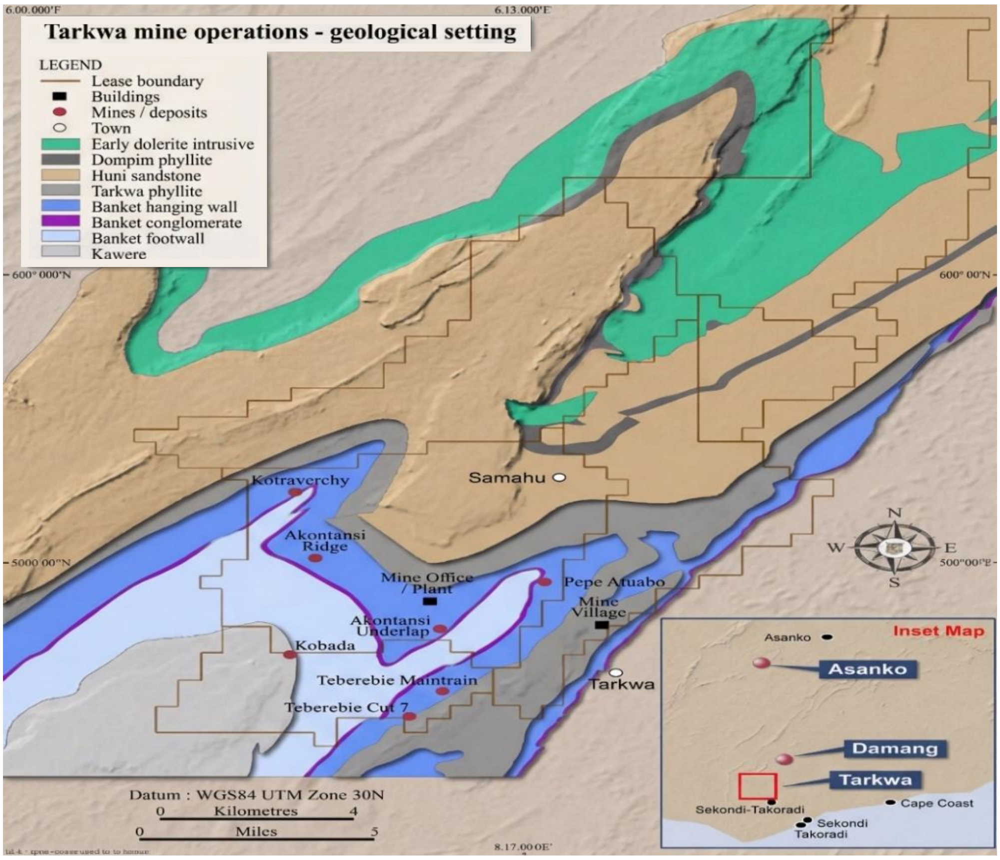

Figure 2. Local geology of Tarkwa Gold Mine area (after [14]).

Geological Setting of the Tarkwa Mine

The Tarkwa mine is dominated by the Banket Series, consisting of footwall and hanging wall barren quartzite, separated by a sequence of mineralized conglomerates and pebbly quartzites (Figure 2). The

© STM Journals 2026. All Rights Reserved

stratigraphy of the quartzite units consists of auriferous reefs interbedded with barren immature quartzites. Structurally, the Tarkwaian belt has been subjected to moderate folding. Also, the ore bodies are cut by numerous faults, which generally run perpendicular to the strike and are predominantly reverse faults. A number of igneous intrusions also cut the reef ore bodies and can cause areas to be sterilized in Figure 2.

MATERIALS AND METHODS

Geological Field Mapping

The pits in Goldfields Ghana Limited, Tarkwa, contain various structures of varying degrees of attitudes. Therefore, rock face mapping was conducted by the author based on the ASTM (American Society for Testing and Materials) and ISRM (International Society for Rock Mechanics and Rock Engineering) standards. The purpose was to assess the walls to identify major structures that could impact slope stability. Also, it is aimed at determining structural characteristics, possible failure modes, shear zones, geological strength index (GSI), and groundwater seepages on wall surfaces for subsequent numerical modeling. During the mapping, structural attitudes were assessed, felt, measured, and recorded for in-situ or undisturbed structures. The attitudes included: dip, dip direction, weathering, alteration, mineralization, seepage, rock quality designation (RQD), spacing, continuity, roughness, infilling, and joint wall hardness. The dip and dip direction were measured with the structural compass. However, weathering, alteration, seepage, and roughness were qualitatively assessed by inspection and inference from standards. The alteration was assessed based on the natural stains on joint wall surfaces, whereas roughness was assessed based on feelings (micro) by fingers and observable features (macro) on joint wall surfaces. The macro features included: planar, undulating, and stepped; however, the micro features included: slickensides, smooth, and rough. Both spacing and continuity were determined using the tape measure. The RQD was determined for a 100 cm span stretch structure with the same orientation. The structures within the 100 cm stretch, which were less than 10 cm, were ignored, whereas those equal to or greater than 10 cm were summed to give the RQD of that set.

The Geological Strength Index

The rock mass in the Goldfield concession area consists of varying strengths, and therefore, GSI was determined for the various lithologies in the pits. It is an estimate of the rock mass strength and the rock mass deformation modulus. In literature, the GSI system is a description of two factors: rock structure and block surface conditions. Therefore, the GSI was determined using RQD and joint condition, JCond89 [15], adopting the chart [16]. The GSI was used as input to determine Hork-Brown parameters for subsequent numerical modeling. The procedure and guidelines used for the determination of GSI in pits are summarized and presented in Tables 1–3, respectively, in Figures 3–6.

The Hoek-Brown Parameters

The FEM in Rocscience was utilized to numerically estimate the peak and residual values of the Hoek-Brown parameters. The peak Hoek-Brown parameters are: m_b, a, and s, whereas the residual parameters are: m_r, s_r and a_r. The finite element estimates these parameters based on the GSI values, the disturbance factor (D = 1) for controlled large open pit production blasting and overburden removal [17], the joint surface condition (roughness, weathering, and infilling), and block size (joint spacing, joint orientation, number of joint sets, and joint persistence). The results of the peak and residual values of these parameters are presented in Table 5.

The Joint Shear Strength Characteristics

A quantitative characterization of the joints, or joint sets, in order to provide three input parameters, was conducted by the author based on Barton-Bandis criterion. These are: joint surface roughness (*JRC: joint roughness coefficient*), the joint wall compressive strength (*JCS: joint compressive strength*), and an empirically derived estimate of the *residual friction angle* (φ_r). As presented in literature, these three parameters have typical ranges of values from: *JRC* = 0 to 20 (smooth-planar to very rough-undulating), *JCS* = 10 to 200 MPa (weak-weathered to strong, unweathered), and φ_r =20° to 35° (strongly weathered-fresh unweathered).

© STM Journals 2026. All Rights Reserved

Table 1. Input parameters for finite element analysis in Akontasi. (a) Physical properties, elastic constants, and Mohr-Coulomb parameters. (b) Hoek-Brown parameters. (c) Barton-Bandis parameters.

(a) Physical properties, elastic constants, and Mohr-Coulomb parameters

Materials		***Physical property***	***Elastic constants***		***Mohr-Coulomb parameters***		
Material name	*Color*	γ (kN/m^3)	*E* *(kPa)*	v	δ_t *(kPa)*	φ *(Deg)*	*C* *(kPa)*
Oxide		22	300000	0.28	17	29	65
Transition		23.55	9.8e6	0.26			
Transition intrusion		22.5	200000	0.39			
Fresh quartzite		27	2.3e6	0.19			
Fresh intrusion		24.9	3.5e6	0.38			
Fresh conglomerate		27.1	2e6	0.22			

(b) Hoek-Brown parameters

Material name	*Color*	*UCS* *(kPa)*	m_b	m_{br}	s	s_r	a	a_r
Oxide								
Transition		75000	2.90711	2.90711	0.011109	0.011109	0.501071	0.501071
Transition intrusion		40000	2.88148	2.88148	0.018316	0.018316	0.500838	0.500838
Fresh Quartzite		150000	3.35355	3.35355	0.015504	0.015504	0.500911	0.500911
Fresh intrusion		90000	3.09483	3.09483	0.021637	0.021637	0.500771	0.500771
Fresh conglomerate		148000	4.06196	4.06196	0.021637	0.021637	0.500771	0.500771

(c) Barton-Bandis parameters

Joint	*Color*	φ_r	*JCS* *(kPa)*	*JRC*	*Kn* *(kPa/m)*	*Ks (kPa/m)*
Joint 1		28	65000	9	20000	15000

Joint Roughness Coefficient

As stated by Barton (2023) [18], roughness is an essential component of the shear strength of rock joints, particularly in the case of unfilled joints. In literature, among the joint roughness parameters, the joint roughness coefficient (JRC) is the most widely used in practice. It is used for evaluating rock joint shear strength and quantifying roughness and, therefore, is adopted by the standards for the description of discontinuities [18]. The conventional visual comparison method was adopted by the author for the estimation of *JRC*. It was done by using the mapped rock faces as presented in Tables 1–3 and in comparison with the adopted roughness profile [19]. Authors acknowledged this approach as it surpasses the experimental methods, e.g., direct shear test, tilt test, and push or pull test) and the amplitude/length test, as these methods are subject to experimental and human errors in measurement.

Joint Compressive Strength

The author adopted the Schmidt rebound hammer approach to estimate the joint compressive strength (JCS) as proposed [20], illustrated in Figure 3 using the adopted [21] standards. During the field estimation of JCS, the standard type-L hammer was used. About twenty (20) rebound readings were taken along horizontal impact surfaces, to avoid normalization due to non-horizontal (gravitational effects) impact directions [22]. The data reduction process was carried out by removing the lowest readings attributed to the presence of hidden cracks and averaging the others by the author. Each impact point was separated by at least two plunger diameters. The mean values were used to estimate the JCS using the adopted [20] chart.

© STM Journals 2026. All Rights Reserved

Table 2. Input parameters for finite element analysis in Pepe: (a) physical properties, elastic constants, and Mohr-Coulomb parameters, (b) Hoek-Brown parameters, (c) Barton-Bandis parameters.

(a) Physical properties, elastic constants, and Mohr-Coulomb parameters							
Materials		***Physical property***	***Elastic constants***		***Mohr-Coulomb parameters***		
Material name	*Color*	γ $(KN/m^3$	*E* *(kPa)*	v	δ_t *(kPa)*	φ *(Deg)*	*C* *(kPa)*
Oxides		22	2.8e6	0.29	25	28	60
Transition quartzite		23.9	1.15e7	026			
Intrusion dolerite		25	7e6	0.32			
Fresh quartzite		26.5	2.4e6	0.19			
Fresh conglomerate		26	1.95e7	0.21			

(b) Hoek-Brown parameters								
Material name	*Color*	*UCS (kPa)*	m_b	m_{br}	s	s_r	a	a_r
Oxides								
Transition quartzite		74000	2.70671	2.70671	0.009404	0.009404	0.50116	0.50116
Intrusion dolerite		90000	4.11832	4.11832	0.042144	0.042144	0.500541	0.500541
Fresh quartzite		145000	3.86853	3.86853	0.021637	0.021637	0.500771	0.500771
Fresh conglomerate		143000	5.4053	0.590429	0.042144	0.00024	0.500541	0.505734

(c) Barton-Bandis parameters						
Joint	*Color*	φ_r	*JCS (kPa)*	*JRC*	*Kn (kPa/m)*	*Ks (kPa/m)*
Joint 1		28	65000	9	100000	10000
Joint 2		28	65000	9	100000	10000
Minor fault		15	15000	9	100000	10000

Residual Friction Angle (φ_r)

The tilt test approach was used to estimate the residual friction angle (φ_r) of joints in the open pits based on the study by Barton (2014) [23]. In the test, the tilt angle (α) of joint sets was first estimated. Two blocks forming the joint were extracted gently from the rock mass in each pit. The upper block was weighed gently with a balance, and the contact area was estimated. One block (upper block) was placed on top of the other (lower block), with the joint resting on a horizontal plane. The two-block set was made to progressively turn, but prevent the interaction with the upper block, the one that will have to be in contact according to its own weight, without external forces. An angle measurement was done with a compass on the joint. Once the upper block started to slide, the test was stopped.

The angle between the joint and the horizontal plane gives the angle of inclination α. Equation (1) below was then used to estimate the residual friction angle. The estimation was done on two different joint sets to obtain the average residual friction angle.

$$JRC = \frac{\alpha - \varphi_r}{log_{10}\frac{JCS}{a_{no}}} \quad (3)$$

Where,
JRC is the joint roughness coefficient
α is the joint tilt angle

JCS is the joint compressive strength and a_{no} is the normal stress on the joint corresponding to the normal component of the weight divided by the apparent contact area.

© STM Journals 2026. All Rights Reserved

Table 3. Input parameters for finite element analysis in Teberebie: (a) physical properties, elastic constants and Mohr-Coulomb parameters, (b) Hoek-Brown parameters, (c) Barton-Bandis parameters.

(a) Physical properties, elastic constants, and Mohr-Coulomb parameters

Materials		*Physical property*	*Elastic constants*		*Mohr-coulomb parameters*		
Material name	*Color*	γ (kN/m^3	*E (kPa)*	v	δ_t *(kPa)*	φ *(Deg)*	*C (kPa)*
Oxides		22	2.8e6	0.28	25	31	60
Transition quartzite		24	1.2e7	0.22			
Intrusion dolerite		26	1.12424e7	0.32			
Fresh quartzite		26	2.5e7	0.22			
Fresh conglomerate		27	1.9e7	0.20			

(b) Hoek-Brown parameters

Material name	*Color*	*UCS (kPa)*	m_b	m_{br}	s	s_r	a	a_r
Oxides								
Transition quartzite		75000	2.34638	0.211283	0.006738	0.000123	0.501355	0.507551
Intrusion dolerite		120000	1.877111	0.98696	0.006738	0.001503	0.501355	0.502644
Fresh quartzite		150000	1.2337	1.2337	0.001503	0.001503	0.502644	0.502644
Fresh conglomerate		160000	3.52122	3.52122	0.015504	0.015504	0.500911	0.500911

(c) Barton-Bandis parameters

Joint	*Color*	φ_r	*JCS (kPa)*	*JRC*	*Kn (kPa/m)*	*Ks (kPa/m)*
Joint 1		28	65000	9	20000	15000

Joint Normal Stiffness (K_n) and Shear Stiffness (K_s)

The finite element in Rocscience numerically estimates the normal and shear stiffness of the joints based on *JRC*, *JCS,* and φ_r, adopting the Barton-Bandits slip criterion. The results of K_n and K_s are summarized and presented in Table 5.

FINITE ELEMENT MODELING

The author performed finite element analysis (FEA) utilizing Rocscience, *RS2*, which is capable of calculating stress and strain distributions and displacements at various stages of mining. The purpose of the FEA was to determine the critical stress reduction factor SRF and the total displacement of the rocks on the pit faces, in addition to evaluating stress and strain distributions. This would determine the overall stability conditions of the pits. Also, it is aimed to provide slope stability counter measures in order to avert any slope failure catastrophe.

The FEA was carried out at the hanging walls in order to ascertain the overall slope stability conditions. Studies reported that joints form the final phase of deformation in the concession area. Two sets of near-vertical joints have been identified, striking north-south (NS) and east-west (EW), the former being open and the latter having quartz infill. A third, less well-developed set of joints striking north-west (NW) is also found in Teberebie. These combinations of joint orientation and bedding plane dip may result in bench and high wall stability problems.

These structural characteristics, as identified during field mapping, warranted the hanging wall slope stability analyses. However, the footwall, which is relatively gentle and stable, is being used for the waste rock dump.

© STM Journals 2026. All Rights Reserved

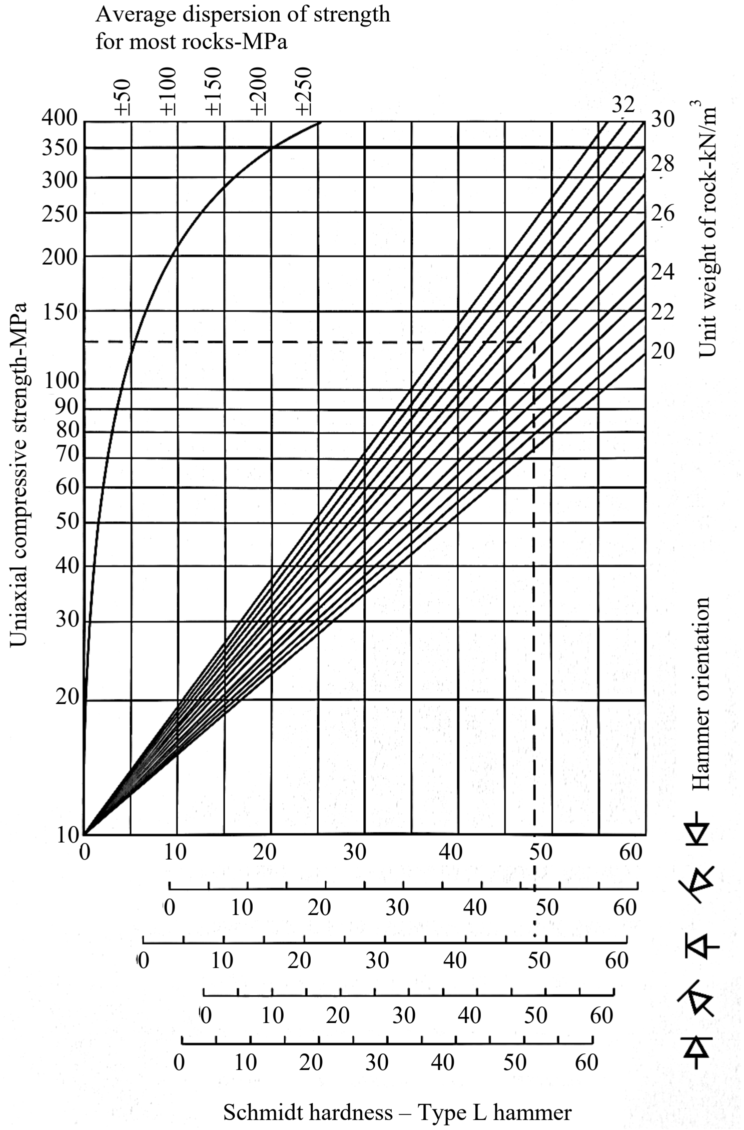

Figure 3. Estimate of joint wall compressive strength from Schmidt hammer rebound hardness (adopted [20]).

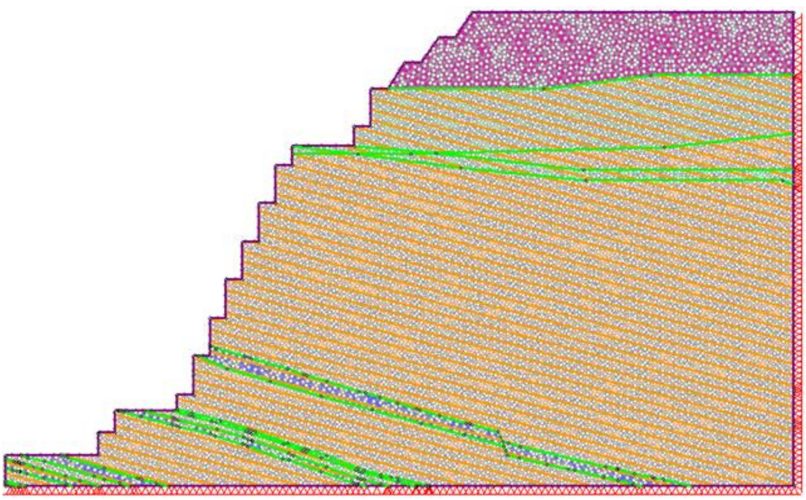

Figure 4. Established geometrical model of Akontasi pit.

Journal of Geotechnical Engineering
Volume 13, Issue 1
ISSN: 2394-1987

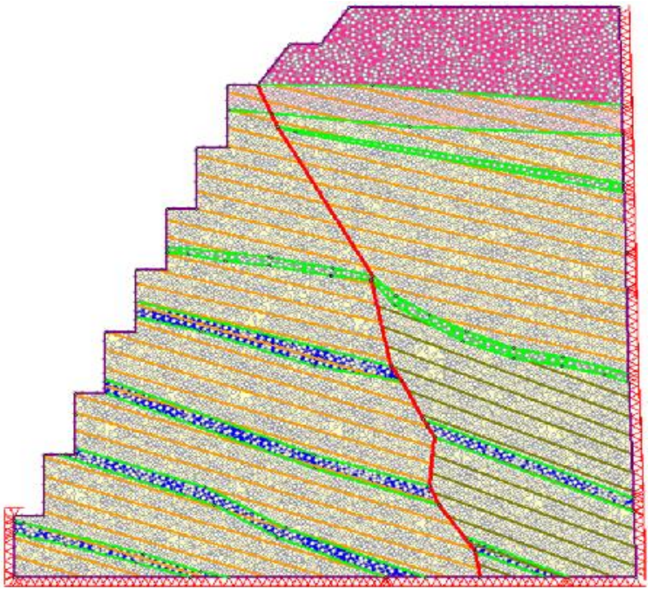

Figure 5. Established a geometrical model of the Pepe pit.

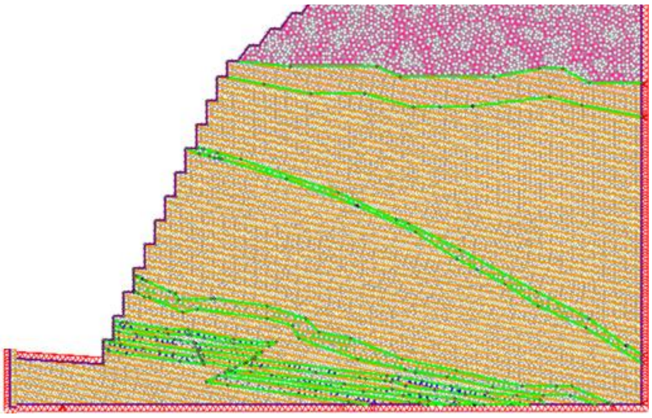

Figure 6. Established a geometrical model of the Teberebie pit.

As indicated by Zienkiewicz (2005) [24], finite element is one of a continuum of problems such that the continuum is divided into a finite number of elements, the behavior of which is specified by a finite number of parameters. As pointed out by Blachowski and Ellefmo (2012) [25], the general form of the FEM includes discretization of the continuum into a finite number of elements, analysis of particular elements of the discrete, formulation and solving a set of equations describing the model, and calculations of displacement, stress, and strain values. In view of this, three established models, as presented in Figures 4–6, were used for the finite element analyses of the pits in Akontasi, Pepe, and Teberebie, respectively. These models consist of quartzite, conglomerate, and intrusion as materials in the three zones of mining.

These mining zones are the oxides (heavily weathered zone), transition zone (slightly weathered), and fresh rocks (unweathered).

For the oxides, the slope angle is 55° with a bench width of 8 m and a bench height of 12 m. Likewise, both the transition and the fresh rocks have slope angles of 90° each with a bench width of 8 m and a bench height of 18 m each, as indicated in the models below.

The input parameters used for FEA consist of shear strength properties of intact core specimens, physical properties of intact core specimens, and shear strength of joints (Tables 1–3).

© STM Journals 2026. All Rights Reserved

CASE STUDY APPLICATION

Data Description

The slope faces have three sets of structures based on their orientations. These joint sets are sub-vertical structures as observed in their dip amounts. The predominant structures have a dip and dip direction of about 85°/220 dipping favorably into the pit faces. The slope faces are dry, and there is no evidence of groundwater seepage within structures except at Teberebie, where there are isolated cases of moist conditions. These sub-vertical structures may be responsible for wedge and toppling failures as evidenced on the pit faces. The structures are typically straight, planar, and slightly rough with a maximum continuity length dip and strike of about 12 m and 10 m, respectively.

As presented in Tables 4, 5, and 6, the RED sandstone and GSI obtained from the slope faces suggest that the lithologies are generally good and highly competent, rough, slightly weathered, with iron-stained surfaces.

Table 4. GSI in Acontias.

Lithology	**Conglomerate**			**Quartzite**		**Intrusive**	
RED%	80	75	70	75	70	80	75
0.5RQD%	40	37.5	35	37.5	35	40	37.5
Weathering	Slightly	Slightly	Slightly	Slightly	Slightly	Moderately	Moderately
Alteration	Slightly	Slightly	Slightly	Slightly	Slightly	Slightly	Slightly
Roughness	Slightly	Slightly	Slightly	Slightly	Slightly	Slightly	Slightly
JCond89 (Bieniawski, 1989)	25	25	25	25	25	25	25
1.5JCond89	37.5	37.5	37.5	37.5	37.5	37.5	37.5
GSI	77 (App. A1a)	75 (App. A1b)	72 (App. A1c)	75 (App. A2a)	72 (App.A2b)	77 (App. A3b)	75 (App. A3a)

Table 5. GSI in Pepe.

Lithology	**Conglomerate**	**Quartzite/quartz vein intrusive**		
RQD%	75	75	66	65
0.5RQD%	37.5	37.5	33	32.5
Weathering	Slightly	Slightly	Slightly	Slightly
Alteration	Slightly	Completely	Completely	Completely
Roughness	Slightly	Slightly	Slightly	Slightly
JCond89 (Bieniawski, 1989)	25	25	25	25
1.5JCond89	37.5	37.5	37.5	37.5
GSI	75 (App. B2a)	75 (App. B1c)	70(App. B1b)	70 (App. B1a)

Table 6. GSI in Teberebie.

Lithology	**Conglomerate**				**Quartzite/Mafic intrusive**			
RQD%	100	90	85	75	75	75	70	70
0.5RQD%	50	45	42.5	37.5	37.5	37.5	35	35
Weathering	Slightly	Slightly	Slightly	Slightly	Slightly	Fresh	Slightly	Fresh
Alteration	Slightly	Slightly	Slightly	Slightly	Slightly	Slightly	Slightly	Slightly
Roughness	Slightly	Slightly	Slightly	Slightly	Slightly	Slightly	Slightly	Slightly
JCond89 (Bieniawski, 1989)	25	25	25	25	25	30	25	30
1.5JCond89	37.5	37.5	37.5	37.5	37.5	45	37.5	45
GSI	90 (App. C2d)	85 (App. C2c)	80 (App. C2b)	75 (App. C2a)	75 (App. C1b)	81.5 (App. C1a)	72 (App. C1c)	80 (App. C1d)

© STM Journals 2026. All Rights Reserved

Moreover, in Teberebie, there are some fresh unweathered surfaces, such as the quartzites, present in some points. In addition, based on the macro and micro roughness scale, the roughness profile obtained in the slope faces in the mine is slightly undulating, planar, and rough. Juxtaposing this to the adopted [19] roughness profile gives an estimated JRC of about 8 to 10 in the mine (Figure 7).

Also, the average rebound number of rocks in Akontasi, Teberebie, and Pepe pits is found to be 37, 36, and 37, respectively. The average rebound number, however, is found to be 2 along the minor fault plane in Pepe. From the adopted [20] chart in Figure 8, the estimated JCS is found to be 65 MPa in the mine pits. Meanwhile, the JCS is found to be 15 MPa along the minor fault plane in Pepe pit, as indicated in Figure 8 and presented in Table 7.

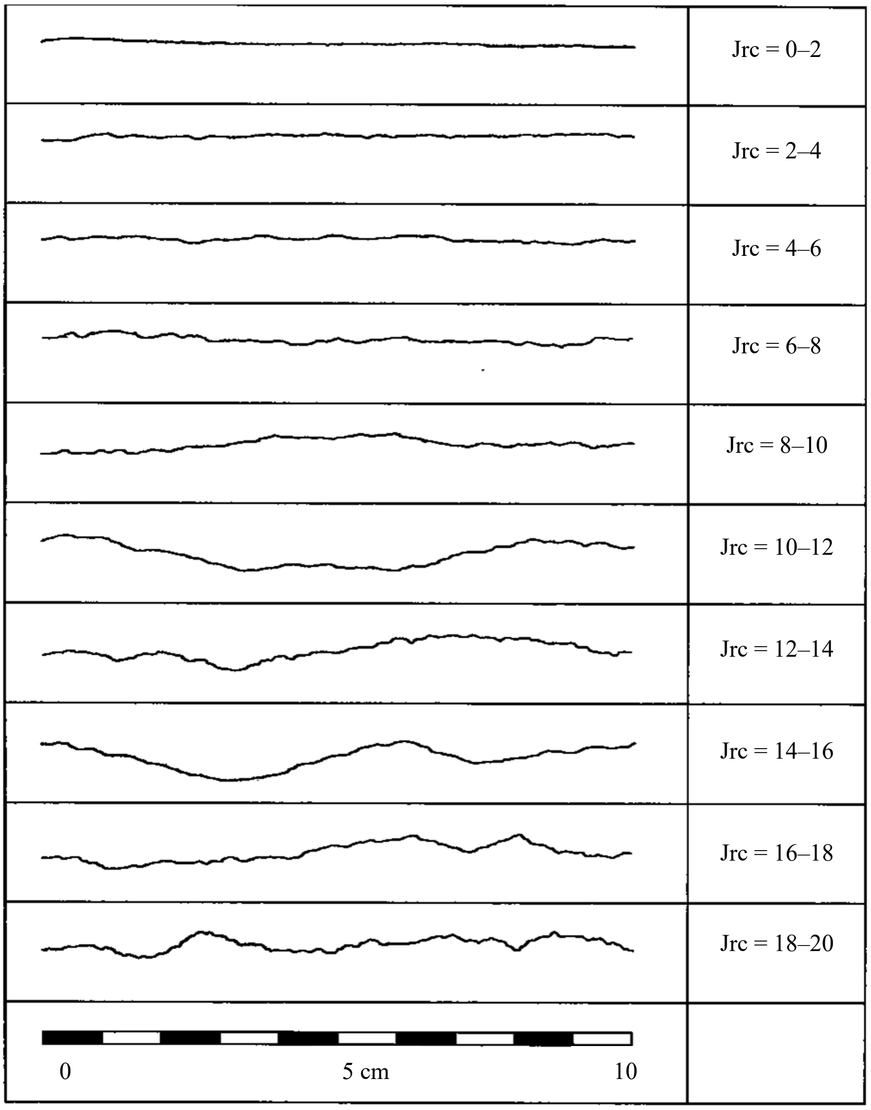

Figure 7. Roughness profile and corresponding JRC values (after [19]).

Table 7. Estimated JCS.

	Rebound number	Unit weight (kN/m^3)	JCS (MPa)
Akpntasi	37	23.5	65
Teberebie	36	24.0	65
Pepe	37	23.5	65
	2	23.5	15

© STM Journals 2026. All Rights Reserved

As stated by Barton et al. (2023) [18], roughness is an essential component of the shear strength of rock joints. The JRC, which is a joint roughness parameter, is used for evaluating rock joint shear strength. Also, JCS, which is dependent on JRC, is a function of joint roughness. The joint roughness characteristics among the rock faces in the pits are similar. They are generally slightly undulating, planar, and rough. This accounted for similar values of JCS and the residual friction angle in the pits. However, due to heavy weathering and shearing along the minor fault zone, its JCS is found to be much smaller (15 MPa) (Figure 8).

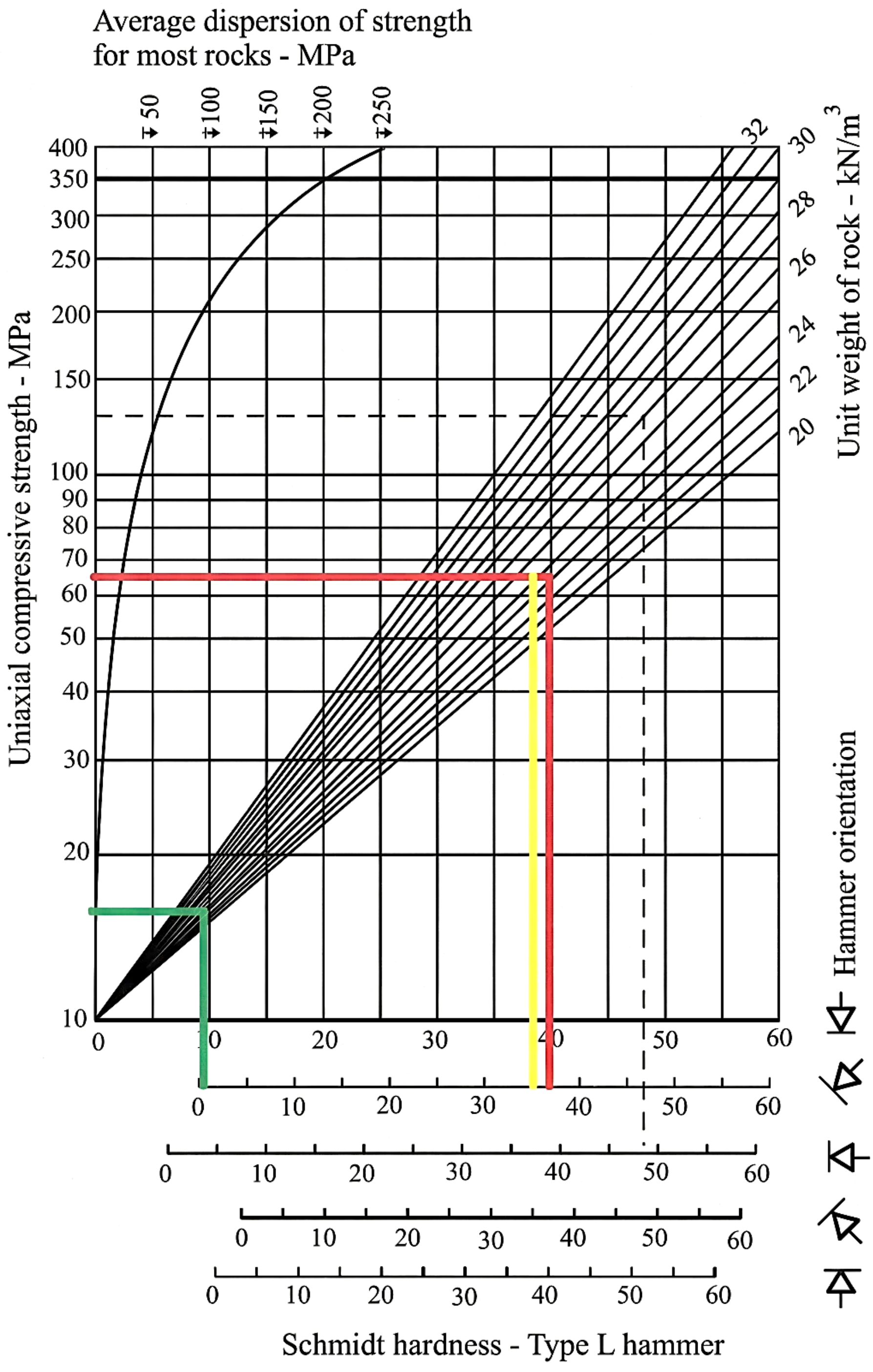

Figure 8. Estimated JCS from [20] Chart (a) Akontasi and Pepe (red), (b) Teberebie (yellow), (c) Pepe minor fault (green). Furthermore, the residual friction angle as presented in Table 8 is on average 28° in the mine pits, indicating highly competent rocks.

© STM Journals 2026. All Rights Reserved

Table 8. Estimated residual friction angle (φ_r).

Pit	Joint	JRC	JCS (MPa)	α	W (kN)	A (cm^2)	a_n $(\frac{W}{A})$ (MPa)	a_{no} $(a_n cos\alpha)$ (MPa)	φ_r (Deg)
Akontasi	Set one	9	65	31	7.0	2.0	35	30.0	28.0
	Set two	9	65	29	9.5	1.8	53	46.5	27.7
Teberebie	Set one	9	65	30	8.8	1.8	49	42	28.3
	Set two	9	65	29.5	9.1	1.8	52	45	28.1
Pepe	Set one	9	65	30	9.0	2.0	45	39	28.0
	Set two	9	65	30.2	9.0	2.0	45	39	28.2
	Fault (minor)	9	65	18.0	6.8	2.0	34	32.5	15.2

Finite Element Analysis

During the FEA, six node triangles were utilized for discretization. The approach utilized the stress reduction factor SRF method to evaluate the critical stress reduction factor (critical SRF) and deformation of rocks in pit faces. During the analysis, field stress and body force were considered as the initial element loading. This is because the stresses were due to both in-situ stresses and stresses due to the surroundings. The surrounding stresses are mining-induced, due to weathering, due to blasting effects, and a change in structural orientation. Additionally, the analyses were conducted independently within the three distinct operational mining zones based on their failure criteria. These zones, thus the oxides, transition zone, and the fresh rocks, have specific and distinct rock properties and failure modes.

In the oxides, the analysis was based on the Mohr-Coulomb criterion since the failure mode was predominantly circular. However, within the transition and the fresh rocks, the analyses were based on the generalized Hoek-Brown criterion since the failure modes were variable (predominantly planar, wedge, and toppling). Furthermore, Barton-Bandis joint slip criterion was considered for modeling the joint shear strength. As stated by Barton (2023) [18], the Barton-Bandis joint model provides a nonlinear shear strength envelope for rock joints and therefore allows the shear strength and normal stiffness of rock joints to be estimated. Moreover, wedge failures were predominantly encountered during the field mapping and were due to sub-vertical joint intersections. For this reason, these joints were considered for the finite element analyses. Also, the Pepe open pit is cut by a number of east-west striking, near-vertical transverse minor faults and therefore illustrated in the Pepe model (Figure 5).

The steps involved in the modeling procedure are constructing a geometrical model based on the mine plan and the geological characteristics of the rock mass, discretizing the model, defining the boundary conditions and stresses, defining and assigning material properties for the three zones in the model, performing calculations, and visualizing and interpreting results. The FEA was performed using input parameters in Tables 4, 5, 6, 7, and 8. Also, the analysis used the shear strength reduction method (SRF) to analyze and evaluate the critical SRF, displacements, and stress and strain distributions around the pit faces. The analysis was done with Rocscience RS2 software.

Models Developed

In the finite element analyses, the models generated consist of horizontal displacement, vertical displacement, total displacement contours, and the maximum shear plastic strain. These models help evaluate stress and strain distribution, slope deformation, and the overall slope stability condition. Specifically, the horizontal, vertical, and total displacement contours determine the deformation rate of the slopes. The strain contours, however, determine the strain distribution around slope faces. The oerall condition of the slopes is, however, ascertained by the critical SRF (Figures 9–12).

© STM Journals 2026. All Rights Reserved

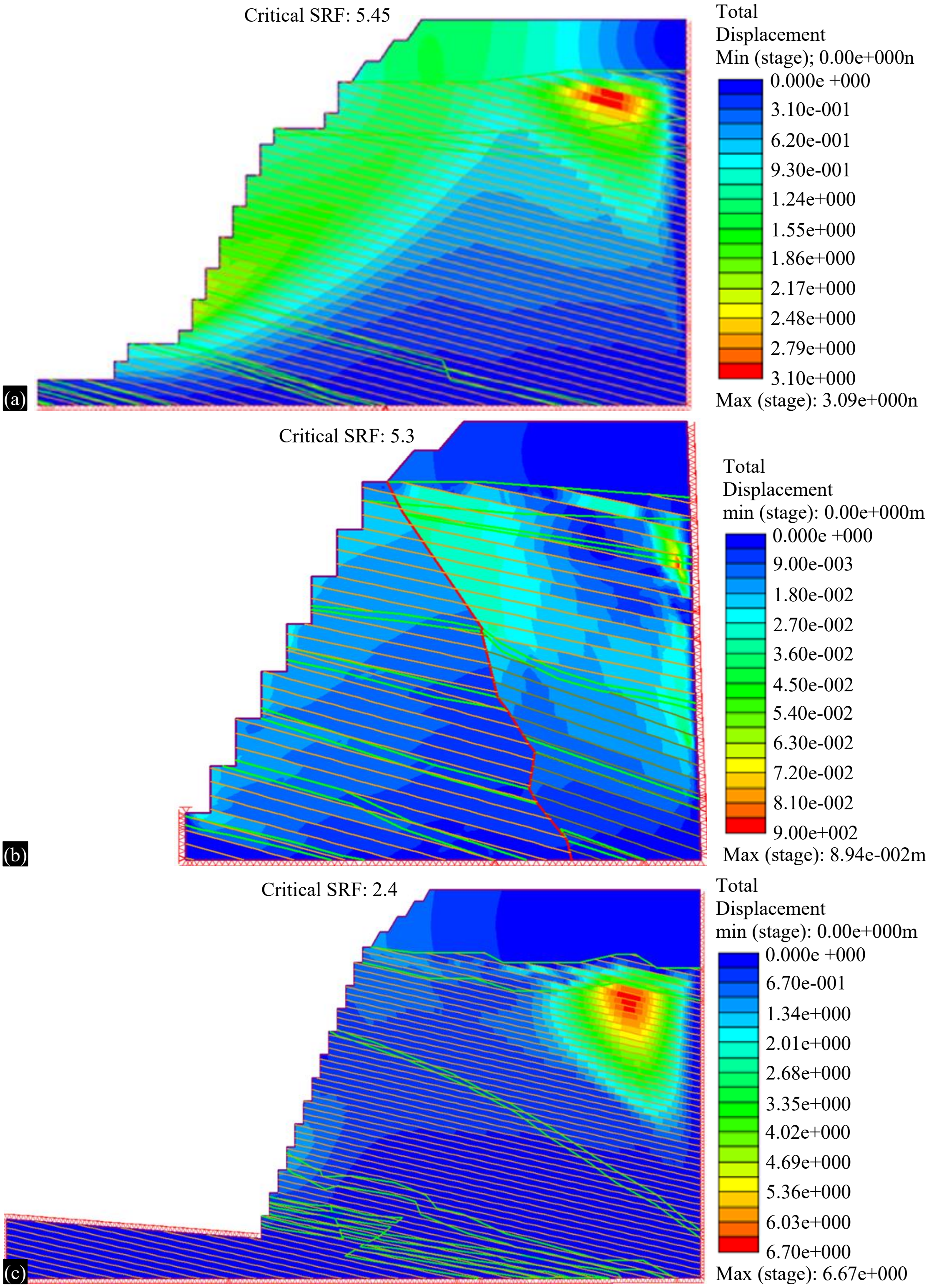

Figure 9. Total displacement contours in (a) Akontasi, (b) Pepe, (c) Teberebie open pit.

Comparison of Models Developed

The FEM is a powerful approach utilized by experts and scholars to assess the stability of slopes under varying stress conditions. The critical SRF obtained from the FEA is a robust variable for inferring the general stability condition of a rock slope. When its value is greater than 1, the slope is stable; otherwise,

ISSN: 2394-1987

it is unstable. From the results, the overall stability conditions of the slopes are very stable in accordance with the planned design, since the critical SRF values are far greater than 1, as depicted in Table 9. The order of stability as obtained from the FEA is Akontasi > Pepe > Teberebie.

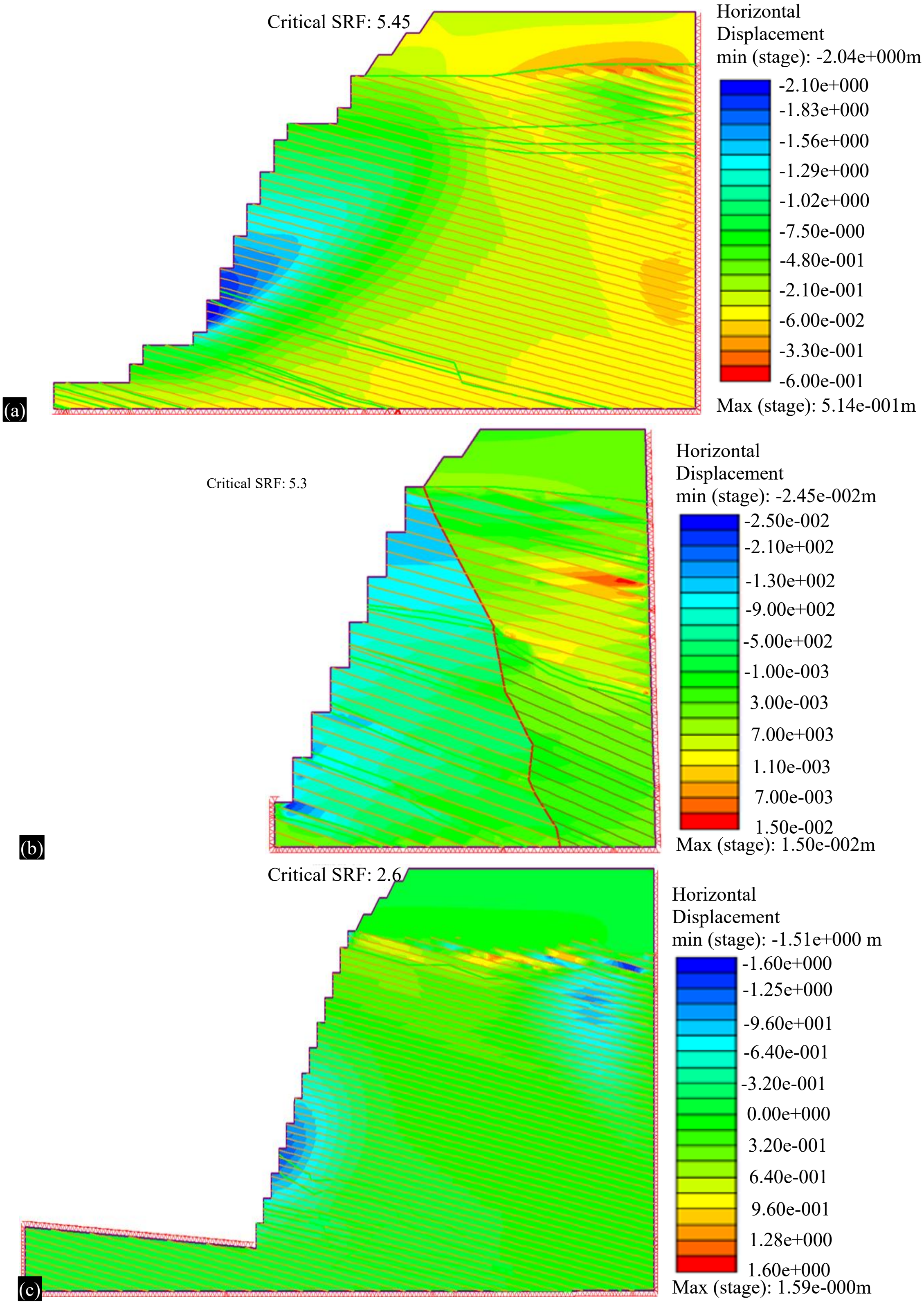

Figure 10. Horizontal displacement contours in (a) Akontasi, (b) Pepe, (c) Teberebie open pit.

© STM Journals 2026. All Rights Reserved

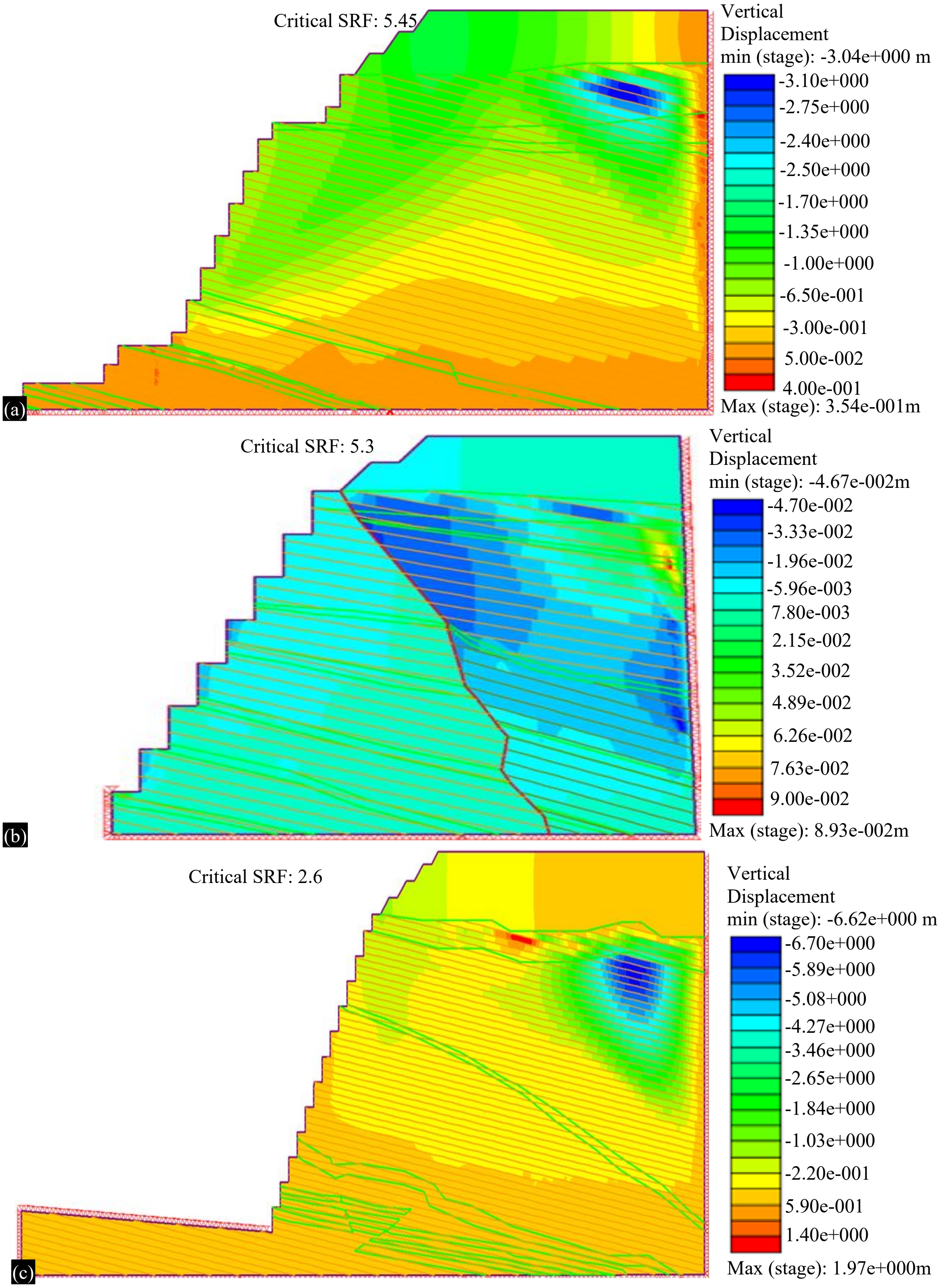

Figure 11. Vertical displacement contours in (a) Akontasi, (b) Pepe, (c) Teberebie open pit.

The high stability of the pit slopes is evidenced by the GSI values and the roughness profile of the structures, which is an indication of strong and highly competent rocks present in the mine slopes. The SRF, however, is influenced by various factors, including: the presence of weak zones, rock stress levels, squeezing or swelling ground conditions, and the rock mass quality. Though the rocks in Teberebie are

© STM Journals 2026. All Rights Reserved

strong and highly competent, it has the lowest SRF value due to the weak zone revealed in the total displacement contour, having a critical displacement of 6.67 m. Also, as shown in Table 9, Teberebie leads with critical horizontal and vertical displacements, in addition to the shear plastic strain.

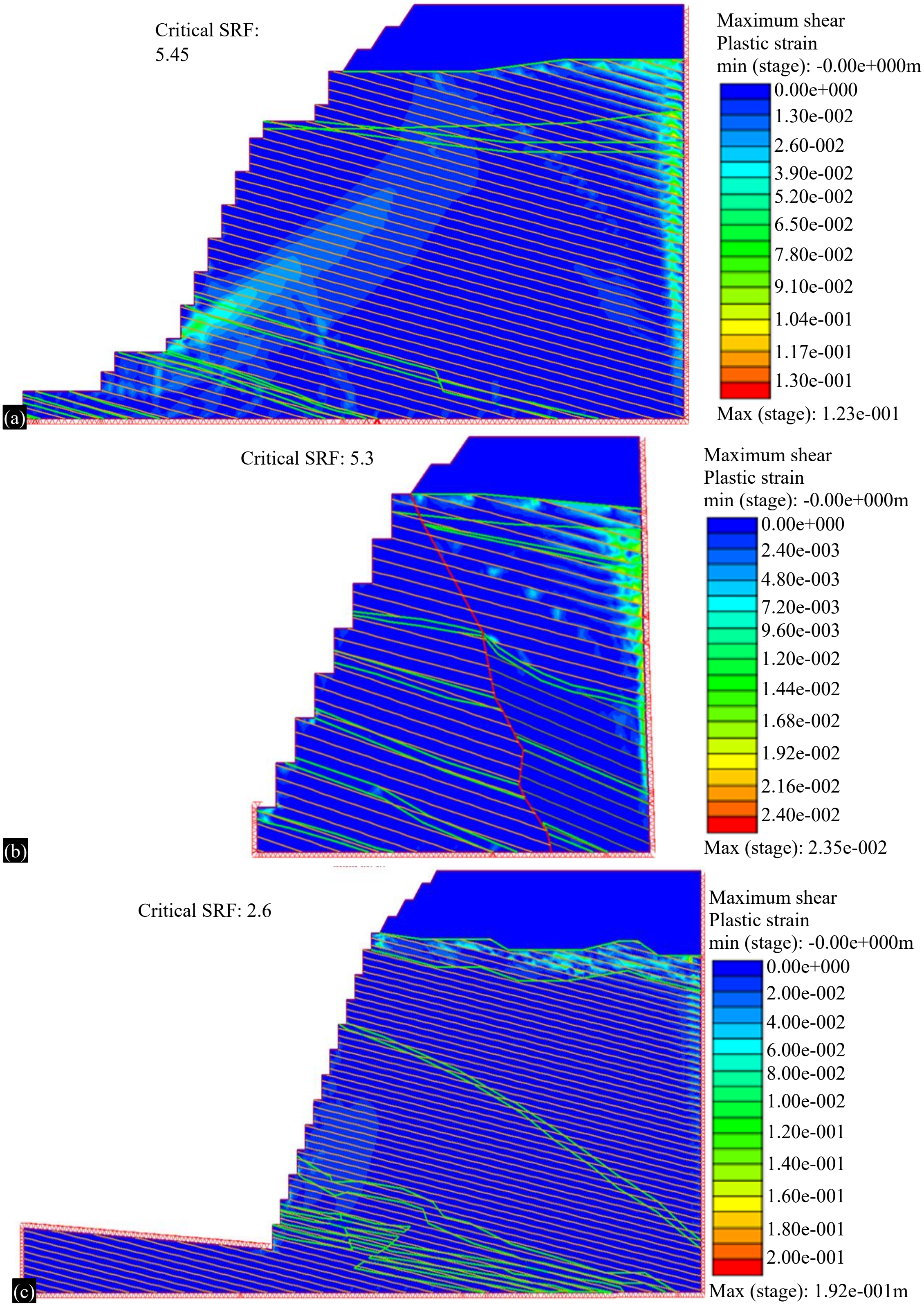

Figure 12. Maximum shear plastic strain contours in (a) Akontasi, (b) Pepe, (c) Teberebie open pit.

© STM Journals 2026. All Rights Reserved

Table 9. Summary of results from the FEA.

Pit	Critical SRF	Critical readings			
		Horizontal displacement (m)	***Vertical displacement (m)***	***Total displacement (m)***	***Shear plastic strain***
Akontasi	5.45	0.541	0.354	3.09	0.123
Pepe	5.3	0.015	0.0893	0.0894	0.0325
Teberebie	2.6	1.59	1.37	6.67	1.92

The displacement contours show the distribution of displacement of structures around the pit faces. These contours reveal the overall deformation patterns, identify potential failure zones, and indicate underlying failure mechanisms such as sliding, settlement, and subsidence. In Akontasi, the benches show some active behavior of total displacement with a potential sliding behavior from the crest to the foot. However, in Pepe and Teberebie, the benches show some regressive behavior in total displacement, illustrating some relative stability of the slope benches. The horizontal and vertical displacements show directional movement of slope structures and are essential to evaluate the directional movement of structures in the slope. These contours indicate the potential for slope instability, identify deformation patterns, and may reveal localized failures. The oxides in the mine pits experienced the highest horizontal displacement, revealing a higher risk of instability. The fresh rocks, however, experienced the highest vertical displacement. The shear plastic strain contours visualized the shear strain distribution around the pit faces. These contours also reveal potential failure zones and strain localization. The contours revealed that the pit slopes have minimal shear strain distribution, illustrating a higher stability of the pit slopes.

VALIDATION WITH LITERATURE

A comprehensive evaluation of an open pit mine was conducted using FEA in Rocscience. The strength reduction factor (SRF) in Rocscience was utilized to assess the stability conditions of the mine slopes. The results unequivocally showed that all the pit slopes are stable with the critical SRF of 5.45, 5.3, and 2.6, respectively, for Akontasi, Pepe, and Teberebie open pits. This is evident from the high GSI values depicting strong and highly competent rocks in the mine pits. The findings underscore the effectiveness of the strength reduction factor in assessing the stability of mine rock slopes. The findings are also consistent with previous studies that have proven effective in mine slope stability assessment. For example, Díaz-Durán [26] found the SRF of an open pit with thin weak layers at various excavation stages to be 3.26, 2.32, and 1.46 during a static evaluation of the slope utilizing the strength reduction factor. Also, Wang et al. (2024) [27] conducted a static stability analysis of the Fushun West open pit mine in China and found the SRF of 1.55. Moreover, You et al. (2018) [28] investigated three slope configurations composing of shale and siltstone formation with some volcanics, for three stage inter ramp angles of 43°, 49° and 54° and obtained the equivalent FOS of 1.96, 1.87 and 1.40 for the generalized Hoek-Brown failure criterion and 2.76, 2.00 and 1.96 for Mohr-Coulomb failure criterion under dry slope for the three configurations, respectively.

LIMITATIONS OF THE STUDY

While this study offers a valuable assessment of the surface mine stability condition from the shear strength reduction analysis, there are several limitations that should be acknowledged. Firstly, the FEA may not fully capture the complex behavior of the rock mass. Uncertainties in input parameters, such as rock properties and in-situ stress conditions, may affect the accuracy of the FEA. Moreover, the choice of mesh size and discretization may affect the accuracy of the FEA (Appendix).

CONCLUSION

FEA was conducted for three (3) open pits in Goldfields Ghana Limited, Tarkwa. The analysis was conducted to ascertain the overall stability conditions of the pits, the deformation, and stress and strain distributions around the pit faces. Results from the overall rock mass stability analyses revealed that the

© STM Journals 2026. All Rights Reserved

design planned for the pits' walls, namely Akontasi, Teberebie, and Pepe, were stable. However, three (3) regimes of deformations were revealed, namely: regressive, active, and critical. Around the pit faces, the deformation was mainly active. Critical deformation was, however, revealed behind the pit faces, illustrating zones of instability. The oxides experienced the highest horizontal displacement, particularly the Akontasi open pit, revealing a higher risk of instability. The fresh rocks, however, experienced the highest vertical displacement as a result of settlement.

Hence, to ensure safe and efficient mining operations and optimize cost-effectiveness, targeted dewatering systems, especially dewatering wells and grout curtains, should be installed in the critical deformation zones to reduce water influxes, infiltration, and seepage into the pits. Also, an effective monitoring system, such as GroundProbe, should be installed to monitor deformations of the pit's faces.

REFERENCES

1. Mirzehi M, Moradi Afrapoli A. Sustainable long-term production planning of open pit mines: An integrated framework for concurrent economical and environmental optimization. Resour Policy. 2024;94:105131. doi:10.1016/j.resourpol.2024.105131.
2. Rajendra Kumar PR, Muthukkumaran K, Sharma C. Technological advancements and sustainable practices in rock slope stability: Critical review. Phys Chem Earth A/B/C. 2024;136:103699. doi:10.1016/j.pce.2024.103699.
3. Xu X, Zhu Z, Ye L, Gu X, Wang Q, Zhao Y, et al. Ultimate pit limit optimization method with integrated consideration of ecological cost, slope safety and benefits: A case study of Heishan open pit coal mine. Sustainability. 2024;16:5393. doi:10.3390/su16135393.
4. Pathan SM, Pathan AG, Siddiqui FI, Memon MB, Soomro MHAA. Open pit slope stability analysis in soft rock formations at Thar coalfield Pakistan. Arch Min Sci. 2022;67(3):437-454. doi:10.24425/ams.2022.142409.
5. Affam M, Balegha M. Geotechnical modeling of optimal pit: West limb of the Tarkwaian of Ghana. Ghana Min J. 2022;22(1):1-8. doi:10.4314/gm.v22i1.1.
6. Steiakakis E, Xiroudakis G, Lazos I, Vavadakis D, Bazdanis G. Stability analysis of a multi-layered slope in an open pit mine. Geosciences. 2023;13:359. doi:10.3390/geosciences13120359.
7. Raghuvanshi TK. Plane failure in rock slopes – A review on stability analysis techniques. J King Saud Univ Sci. 2019;31:101-109. doi:10.1016/j.jksus.2017.06.004.
8. Usmani A, Pal S, Nanda A. Continuum and discontinuum analysis of rock caverns. Indian Geotech J. 2018:1-14. doi:10.1007/s40098-018-0322-6.
9. Lu R, Wei W, Shang K, Jing X. Stability analysis of jointed rock slope by strength reduction technique considering ubiquitous joint model. Adv Civ Eng. 2020;2020:8862243. doi:10.1155/2020/8862243.
10. Pigois JP, Groves DI, Fletcher IR, McNaughton NJ, Snee LW. Age constraints on Tarkwaian palaeoplacer and lode-gold formation in the Tarkwa-Damang District, SW Ghana. Miner Deposita. 2003;38:695-714. doi:10.1007/s00126-003-0360-5.
11. Seidu M, Andrews PG, Acheampong C, Conduah E. Steepened open pit slopes can be stable: Case studies of Gold Fields, Ghana. In: SSIM 2023; Perth, Australia. Perth: Australian Centre for Geomechanics; 2023. p. 577-594. doi:10.36487/ACG_repo/2335_38.
12. Avane GB, Saayman AF. Tarkwa Gold Mine, Ghana, West Africa – A case example of upgrading the reliability of reserves by improved accounting for structural geology in pit designs. In: Potvin Y, editor. Slope Stability 2007: Proceedings of the 2007 International Symposium on Rock Slope Stability in Open Pit Mining and Civil Engineering; 2007; Perth, Australia. Perth: Australian Centre for Geomechanics; 2007. p. 117–128. doi:10.36487/ACG_repo/708_6.
13. Seidu J, Ewusi A. Assessment of groundwater quality using hydrogeochemical indices and statistical analysis in the Tarkwa mining area of Ghana. J Environ Hydrol. 2018;26(Paper 1):1–14.
14. Verbeek J, Butcher R. Technical Report – National Instrument 43-101: Tarkwa Gold Mine, Ghana, West Africa. Gold Fields Limited; 2022. Available from: https://minedocs.com/23/Tarkwa-TR-12312021.pdf

© STM Journals 2026. All Rights Reserved

15. Bieniawski ZT. Engineering Rock Mass Classifications: A Complete Manual for Engineers and Geologists in Mining, Civil and Petroleum Engineering. New York: John Wiley & Sons, Inc.; 1989.
16. Hoek E, Carter TG, Diederichs MS. Quantification of the geological strength index chart. In: Proceedings of the 47th US Rock Mechanics/Geomechanics Symposium; 2013 Jun 23–26; San Francisco, CA, USA. Alexandria (VA): American Rock Mechanics Association; 2013.
17. Hoek E, Brown ET. The Hoek-Brown failure criterion and GSI. J Rock Mech Geotech Eng. 2018:1-19.
18. Barton N, Wang C, Yong R. Advances in joint roughness coefficient (JRC) and its engineering applications, a review. J Rock Mech Geotech Eng. 2023;15:3352-3379.
19. Barton NR, Choubey V. The shear strength of rock joints in theory and practice. Rock Mech. 1977;1-2:1-54.
20. Deere DU, Miller RP. Engineering Classification and Index Properties of Rock. Technical Report No. AFNL-TR-65-116. Albuquerque (NM): Air Force Weapons Laboratory; 1966.
21. ISRM. Suggested methods for the quantitative description of discontinuities in rock masses. Int J Rock Mech Min Sci Geomech Abstr. 1978;15:319-368.
22. Aydin A, Basu A. The Schmidt hammer in rock material characterization. Eng Geol. 2005;81:1-14. doi:10.1016/j.enggeo.2005.06.
23. Barton N. Shear strength of rock, rock joints, and rock masses: Problems and some solutions. In: Alejano LR, Perucho A, Olalla C, Jiménez R, editors. Rock Engineering and Rock Mechanics: Structures in and on Rock Masses. London: Taylor & Francis; 2014. p. 3-16.
24. Zienkiewicz OC, Taylor RL, Zhu JZ. The Finite Element Method: Its Basis and Fundamentals. 6th ed. Oxford: Butterworth-Heinemann; 2005.
25. Blachowski J, Ellefmo S. Numerical modelling of rock mass deformation in sublevel caving mining system. Acta Geodyn Geomater. 2012;9(3):379-388.
26. Díaz-Durán FA. Slope stability in open pits with thin weak layers. In: RIC 2023; Monterrey, Mexico. Monterrey: Tecnológico de Monterrey; 2023. p. 522-533. doi:10.2991/978-94-6463-258-3_50.
27. Wang T, Yuan L, Bi M. Finite element analysis of slope stability of Fushun west open-pit mine. Tech Gaz. 2024;31(6):1968-1974. doi:10.17559/TV-20231219001218.
28. You G, Al Mandalawi MA, Soliman A, Dowling K, Dahlhaus P. Finite element analysis of rock slope stability using shear strength reduction method. In: Frikha W, Varaksin S, Viana da Fonseca A, editors. Soil Testing, Soil Stability and Ground Improvement: Proceedings of the 1st GeoMEast International Congress and Exhibition, Egypt 2017 on Sustainable Civil Infrastructures. Cham: Springer International Publishing; 2018. p. 227-235. doi:10.1007/978-3-319-61902-6_18.

© STM Journals 2026. All Rights Reserved

APPENDICES

Appendix A

Appendix A1. Determination of GSI of conglomerate in Akontasi (a) RQD = 80% (green), (b) RQD = 75% (black), and (c) RQD = 70% (blue) (Figures A1 and A2).

Appendix A2. Determination of GSI of quartzite in Akontasi (a) RQD =75% (yellow), (b) RQD = 70% (blue).

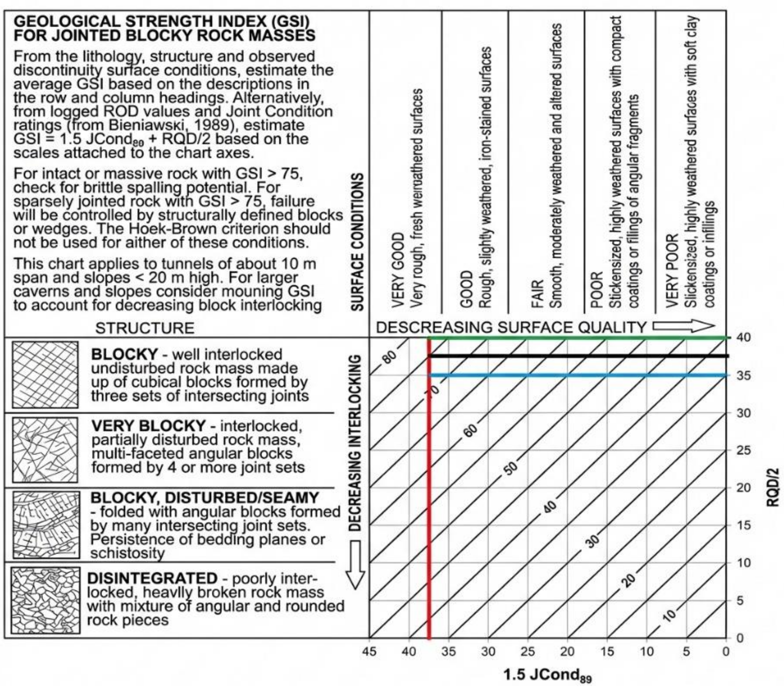

Figure A1. Determination of GSI of conglomerate in Akontasi.

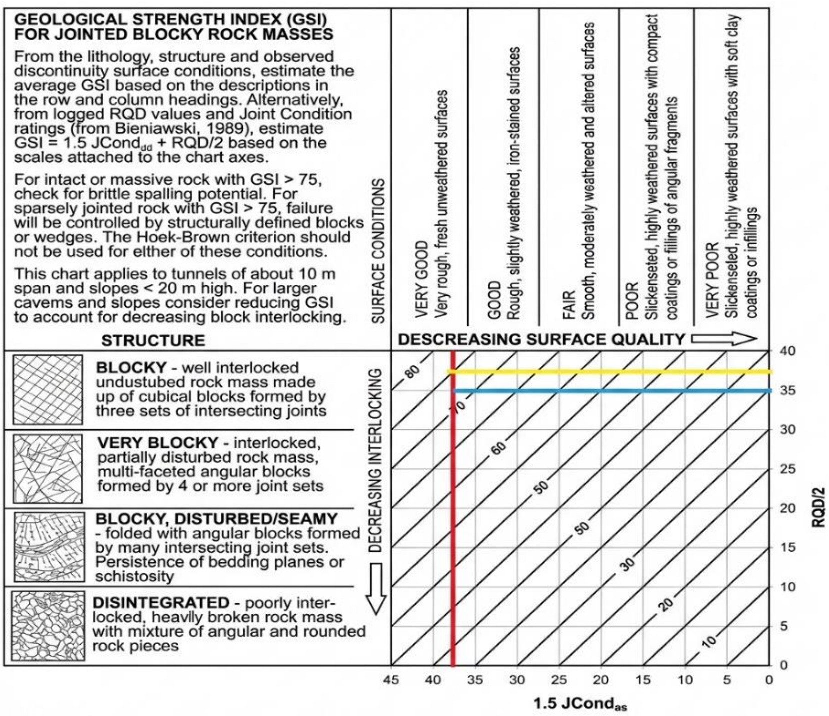

Figure A2. Determination of GSI of quartzite in Akontasi.

Appendix A3. Determination of GSI in intrusive in Akontasi (a) RQD =75% (green), (b) RQD = 80% (blue) (Figure A3).

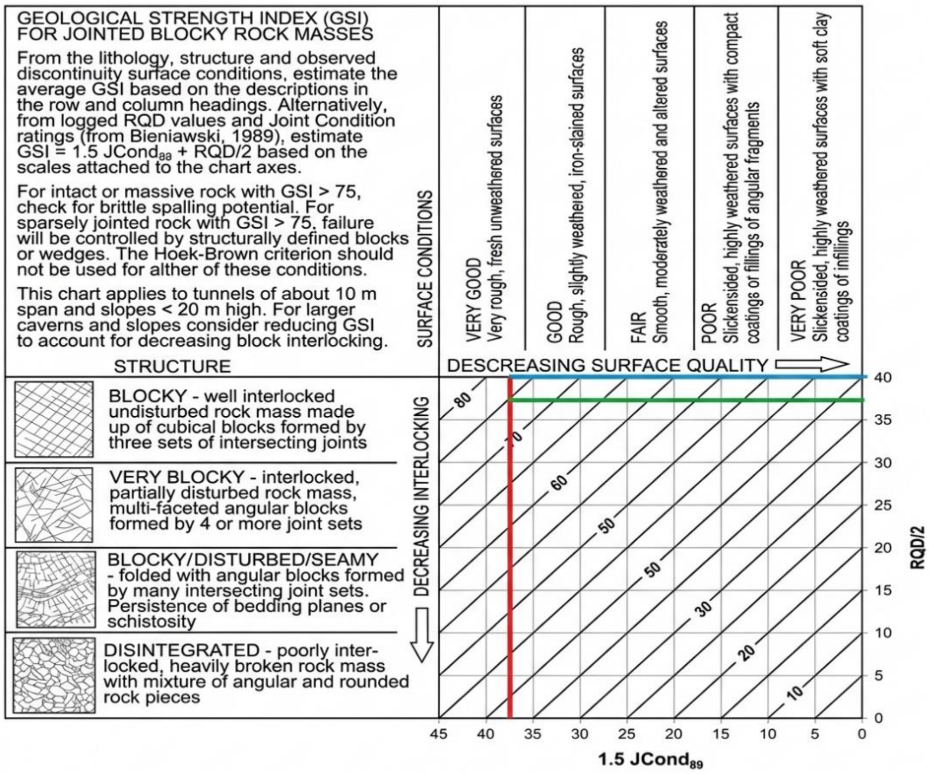

Figure A3. Determination of GSI in intrusive in Akontasi.

Appendix B

Appendix B1. Determination of GSI of quartzite/quartz vein in Pepe (a) RQD =65% (green), (b) RQD = 66% (black), (c) RQD = 75% (blue) (Figure B1).

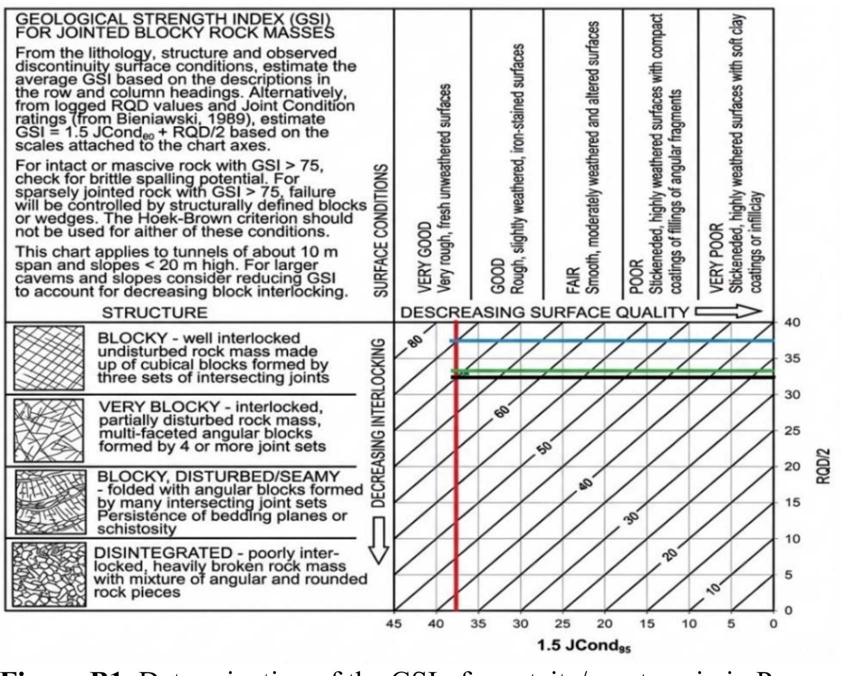

Figure B1. Determination of the GSI of quartzite/quartz vein in Pepe.

© STM Journals 2026. All Rights Reserved

Appendix B2. Determination of GSI of conglomerate in Pepe (a) RQD = 75% (blue) (Figure B2).

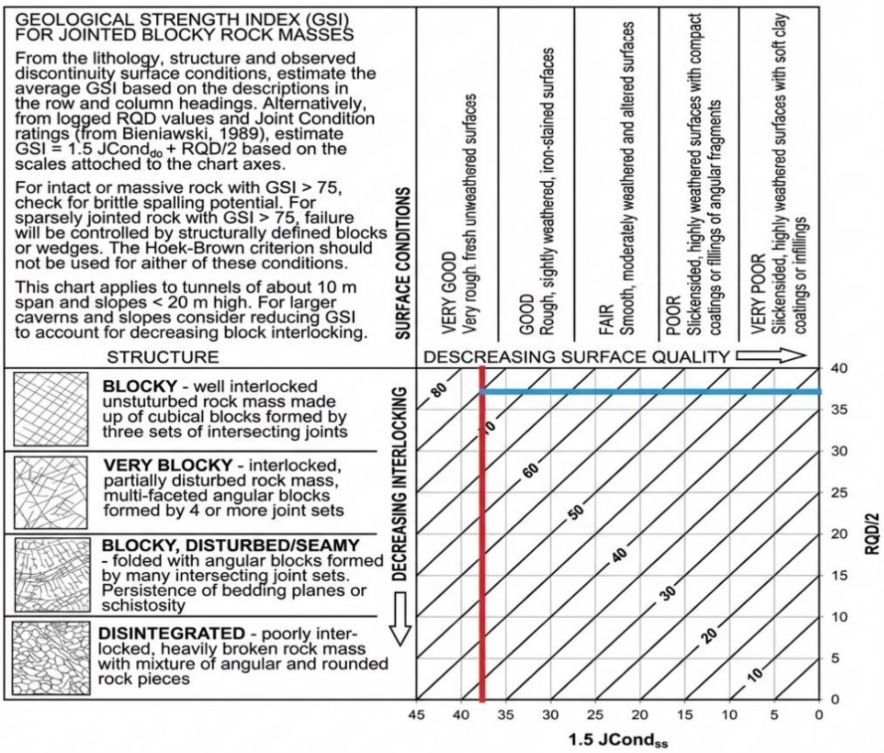

Figure B2. Determination of the GSI of conglomerate in Pepe.

Appendix C

Appendix C1. Determination of GSI of quartzite/mafic intrusion in Teberebie (a) RQD =75% (fresh), (b) RQD = 75% (slightly weathered, (c) RQD = 70% (slightly weathered (d) RQD = 70% (fresh) (Figure C1).

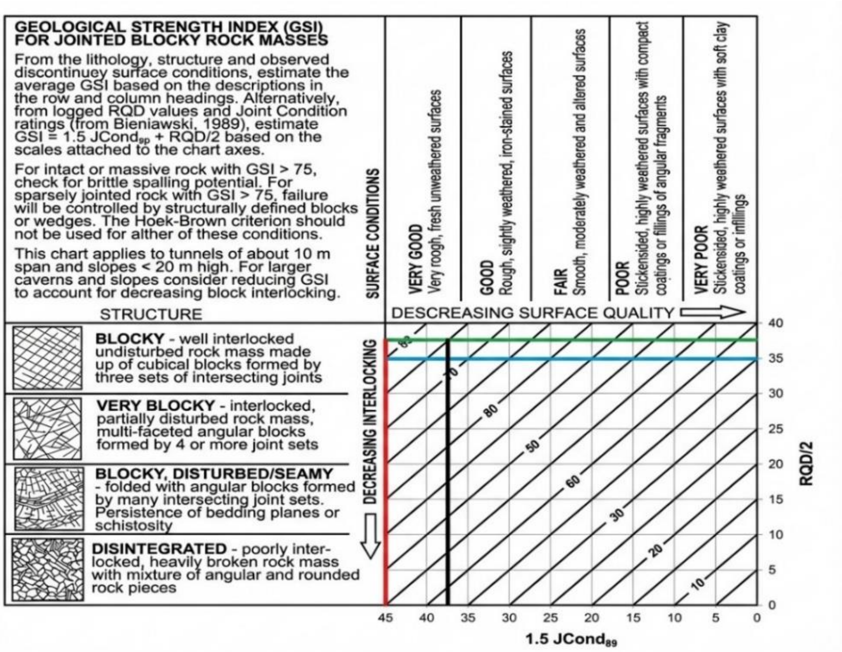

Figure C1. Determination of GSI of quartzite/mafic intrusion in Teberebie.

© STM Journals 2026. All Rights Reserved

Appendix C2. Determination of GSI of conglomerate in Teberebie (a) RQD =75% (yellow), (b) RQD = 85% (green), (c) RQD = 90% (green), (d) RQD = 100% (green) (Figure C2).

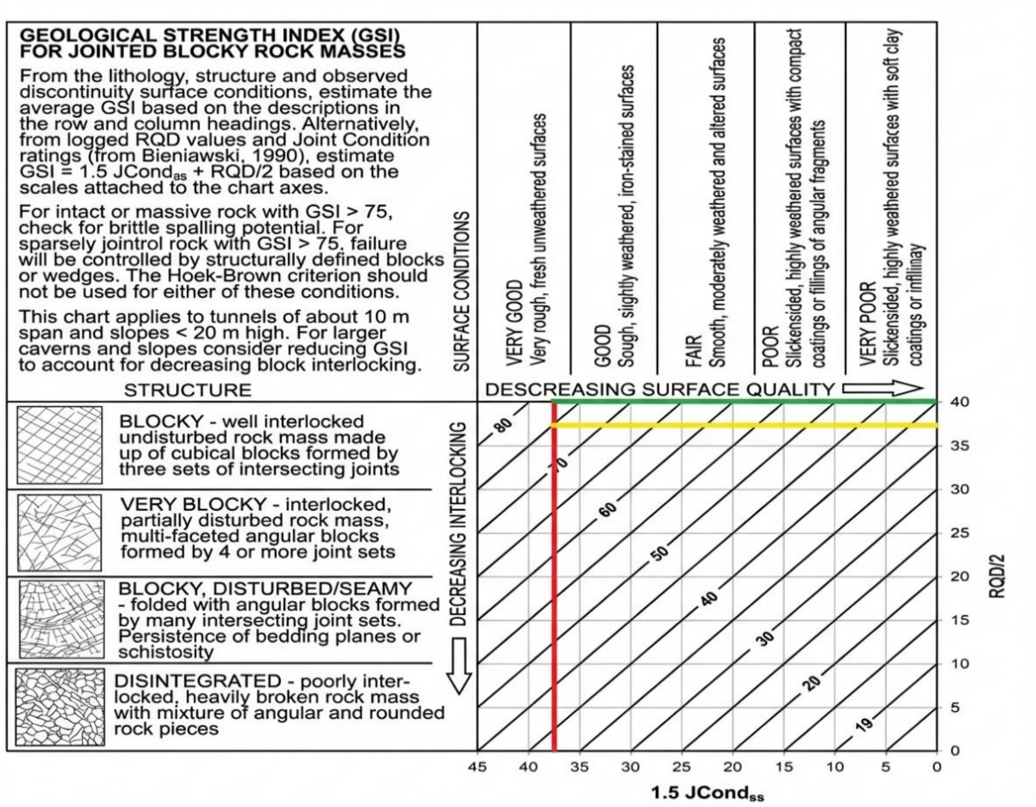

Figure C2. Determination of GSI of conglomerate in Teberebie.